BIOCHEMISTRY
including biophysical chemistry & molecular biology

Article

pubs.acs.org/biochemistry

Involvement of Histidine Residues in the pH-Dependent β-Galactoside Binding Activity of Human Galectin-1

Hirotsugu Hiramatsu,* Katsuyuki Takeuchi, and Hideo Takeuchi

Graduate School of Pharmaceutical Sciences, Tohoku University, Aobayama, Sendai 980-8578, Japan

ABSTRACT: The pH dependence of the β-galactoside binding activity of human galectin-1 (hGal-1) was investigated by fluorescence spectroscopy using lactose as a ligand. The obtained binding constant K_b was 2.94 ± 0.10 mM^{-1} at pH 7.5. The K_b value decreased at acidic pH with a midpoint of transition at pH 6.0 ± 0.1. To elucidate the molecular mechanism of the pH dependence, we investigated the structures of hGal-1 and its two His mutants (H44Q and H52Q) using fluorescence, circular dichroism, UV absorption, and UV resonance Raman spectroscopy. Analysis of the spectra has shown that the pK_a values of His44 and His52 are 5.7 ± 0.2 and 6.3 ± 0.1, respectively. The protonation of His52 below pH 6.3 induces a small change in secondary structure and partly reduces the galactoside binding activity. On the other hand, the protonation of His44 below pH 5.7 exerts a cation−π interaction with Trp68 and largely diminishes the galactoside binding activity. With reference to the literature X-ray structures at pH 7.0 and 5.6, protonated His52 is proposed to move slightly away from the galactoside-binding region with a partial unfolding of the β-strand containing His52. On the other hand, protonated His44 becomes unable to form a hydrogen bond with galactoside and additionally induces a reorientation and/or displacement of Trp68 through cation−π interaction, leading to a loosening of the galactoside-binding pocket. These structural changes associated with His protonation are likely to be the origin of the pH dependence of the galactoside binding activity of hGal-1.

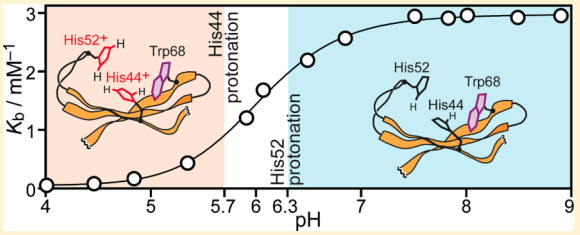

Galectins make up a family of proteins that specifically bind β-galactoside at one or more carbohydrate recognition domains (CRDs) composed of highly homologous amino acid sequences.[1−4] Among many types of galectins, galectin-1 is a prototypic member of the mammalian galectin family that contains one CRD[4,5] and exists predominantly as a noncovalent homodimer under physiological reducing conditions.[6] The dimeric structure of galectin-1 permits simultaneous binding of two molecules of β-galactoside-containing glycoconjugates (glycolipids, glycoproteins, etc.) located at cell surfaces or in extracellular matrices.[5,7−9] The cross-linking of glycoconjugate molecules by galectin-1 is implicated in a wide range of cellular processes such as adhesion, growth, proliferation, and apoptosis of various cells, including immune, inflammatory, and tumor cells.[5,7−12]

Dimeric human galectin-1 (hGal-1) consists of 134 amino acid residues per subunit.[13] An X-ray diffraction study has revealed the crystal structure of a hGal-1 complex with lactose, a β-galactoside in which glucose is linked to galactose through a glycosidic bond.[14] According to the crystal structure, each subunit of hGal-1 is folded into a jellyroll structure composed of two antiparallel β-sheets, one with five and the other with six β-strands. The two β-sheets are curved and overlaid with each other to create a concave pocket for galactoside binding. In the dimeric structure, two galactoside-binding pockets are arranged at the far ends of the dimer with their openings facing in the same direction. A lactose molecule is bound in each galactoside-binding pocket and makes a direct contact with His44, Asn46, Arg48, His52, Asn61, Trp68, Glu71, and Arg73, all of which are conserved in mammalian galectin-1 proteins.[14,15] Site-directed mutagenesis has shown that most of these amino acid residues are essential for producing a high activity of β-galactoside binding.[15,16]

Among the amino acid residues that form the β-galactoside-binding pocket, His44, His52, and Glu71 are pH-responsive. The imidazole side chain of His can be protonated to gain a positive charge with an average pK_a value of 6.6 ± 1.0 in usual proteins.[17] On the other hand, the carboxyl side chain of Glu may be deprotonated to be a negatively charged carboxylate, usually at pH 4.2 ± 0.9.[17] Accordingly, the galactoside binding activity is expected to change with pH in the acidic to neutral region. Actually, the binding activity of hGal-1 shows a peak around pH 7.5−8.0[18] or 6.0−7.8[19] with a steep decrease on the acidic side with a midpoint of transition at pH 5.5−6.5. The decrease in activity at acidic pH may be of biological significance because the in vivo pH value can be as low as ∼5.5 in solid tumors[20−22] and inflammatory tissues[23,24] or below 5 in endosomes and lysosomes.[25,26]

In this study, we have investigated the structural basis of the pH-dependent galactoside binding activity of hGal-1 by examining fluorescence, circular dichroism (CD), and UV Raman spectra of the protein at various pH values in the absence and presence of lactose. Particular attention has been paid to His44 and His52 because the transition pH of the galactoside binding activity so far reported (pH 5.5−6.5)[18,19] is closer to the pK_a value expected for His (6.6 ± 1.0) than that

Received: January 29, 2013
Revised: March 11, 2013
Published: March 19, 2013

for Glu (4.2 ± 0.9). To distinguish the involvement of His44 and His52 in pH-dependent galactoside binding, we have prepared two His → Gln mutants (H44Q and H52Q) and examined the pH dependence of the structure and activity of these mutants to compare them with those of the wild-type protein. The results clearly show that both His44 and His52 induce a decrease in the galactoside binding activity in the protonated cationic state of the side chain, though the protonation of His44 is more influential than that of His52. With reference to X-ray crystal structures in the literature,[14,27] the activity decrease at acidic pH may be explained as follows. Protonated His52 moves slightly away from nearby cationic Arg48 and from the galactoside-binding region, resulting in a reduction in the affinity for galactoside. On the other hand, protonated His44 becomes unable to form a hydrogen bond with galactoside, an essential interaction for the binding of galactoside. Additionally, protonated His44 gives rise to a cation−π interaction with the indole ring of Trp68, inducing a reorientation and/or displacement of the Trp68 indole ring and loosening the galactoside-binding pocket. The His-related pH dependence of the galactoside binding activity of hGal-1 may be biologically relevant in the metastasis of cancer cells and in the endocytosis of hGal-1 and its ligands by leukemic T cells.

MATERIALS AND METHODS

Construction of the Plasmid for Recombinant hGal-1. A full-length cDNA encoding the amino acid sequence of wild-type hGal-1 was prepared from a human lung cDNA library (Takara Bio) following the literature method.[28,29] Custom-made 32-mer and 36-mer deoxyoligonucleotides were used as the sense and antisense primers, respectively, for amplification of the complete hGal-1 gene. The nucleotide sequence of the sense primer was composed of a codon sequence encoding nine N-terminal amino acids of hGal-1 preceded by the initiation codon, while the antisense primer contained a sequence complementary to the codon sequence encoding four C-terminal amino acids followed by a stop codon. These primers were ligated to the target DNA encoding the full amino acid sequence of hGal-1 in the cDNA library. The target DNA was then amplified by polymerase chain reaction (PCR, GeneAmp PCR system 9700, Applied Biosystems). After addition of an adenine nucleotide to the blunt ends, the PCR products were inserted into a pGEM-T Easy vector (Promega). *Escherichia coli* competent cells (XL1-Blue, Stratagene) transformed with the pGEM-T vector were cultured, and the plasmid was extracted. The extracted plasmid of pGEM-T and the pET-15b plasmid (Merck) were digested with the restriction enzymes NdeI and NcoI, to insert the target sequence into pET-15b. Using the pET-15b plasmid, *E. coli* BL21-CodonPlus cells (Stratagene) were transformed. The cloning vectors for the H44Q and H52Q mutants were generated by use of a QuikChange site-directed mutagenesis kit (Stratagene), and the mutations were confirmed by DNA sequencing.

Expression of Recombinant hGal-1. The transformed *E. coli* cells were cultured in Luria-Bertani medium at 37 °C for ∼6 h in the presence of ampicillin. Expression of hGal-1 was induced with 0.1 mM isopropyl β-D-thiogalactopyranoside for 3 h.[29,30] The cells were harvested by centrifugation at 2000*g* for 10 min at room temperature and disrupted with a sonicator (Sonifier250, Branson) in 20 mM phosphate buffer (pH 7.5) containing 150 mM NaCl, 4 mM β-mercaptoethanol (β-ME), 2 mM EDTA, and 1 mM phenylmethanesulfonyl fluoride (a protease inhibitor). Nucleic acids were removed from the cell lysate by centrifugation at 16000*g* and 4 °C for 15 min in the presence of 1% (w/v) streptomycin (Nacalai Tesque). The supernatant was collected as the crude enzyme source.

Purification of the Protein. Wild-type hGal-1 was isolated from the crude enzyme source using an affinity column packed with lactose gel (EY laboratories). Elution of the protein from the column was performed with 20 mM phosphate buffer (pH 7.5) containing 150 mM NaCl, 4 mM β-ME, and 100 mM lactose. The eluate was dialyzed against doubly distilled water, lyophilized, and then purified by gel filtration chromatography (Sephacryl S-100, GE Healthcare). The gel running buffer contained 20 mM phosphate (pH 7.5), 150 mM NaCl, and 4 mM β-ME. Fractions showing absorption at 254 nm were pooled and dialyzed against doubly distilled water to remove nonprotein agents. After lyophilization, the final product was obtained as a white powder with a yield of ∼5 mg/L of culture medium. The purified protein was stored at −80 °C.

The H52Q mutant retained the galactoside binding activity and was isolated and purified by affinity and gel filtration chromatography in the same way as described above for wild-type hGal-1. On the other hand, the H44Q mutant did not show any affinity for galactoside and could not be purified by affinity chromatography. Accordingly, a combination of hydrophobic chromatography on a butyl-Sepharose column (GE Healthcare) and ion-exchange chromatography on a DEAE-cellulose column (DE-52, Whatman) was employed to isolate the H44Q mutant before the final purification by gel filtration chromatography.

Identification of the Purified Protein. The amino acid sequence of recombinant hGal-1 was confirmed by peptide mass fingerprint analysis, in which the protein was digested to fragments with lysyl-endopeptidase and the monoisotopic masses of peptide fragments were determined by time-of-flight mass spectrometry (Voyager DE-STR, Applied Biosystems). The obtained monoisotopic masses were in agreement with those calculated for recombinant hGal-1 having an additional methionine at the N-terminus. The activity of the purified protein as a galectin was assessed by direct hemagglutination of rabbit erythrocytes. The protein was dissolved in 10 mM phosphate buffer (pH 7.2) containing 150 mM NaCl and 4 mM β-ME and then incubated at 4 °C for 48 h to break any disulfide bridges. (hGal-1 loses its galactoside binding activity in the oxidized form containing disulfide bridges.[30]) Solutions containing 0.13−275.0 μg/mL hGal-1 were prepared by serial dilution and were individually mixed with an equal volume of a 2% (v/v) suspension of rabbit erythrocytes. The mixture solution was incubated for 1 h at room temperature in a test tube, and the hemagglutination was judged from the formation of a buttonlike aggregate at the bottom of the test tube. The hGal-1 protein of this preparation was found to agglutinate erythrocytes at a concentration of ≥2.1 μg/mL, which was comparable to a literature value (≥6.25 μg/mL).[30] This observation confirmed the proper folding of the recombinant hGal-1 protein used in this study.

Sample Preparation for Spectroscopic Measurements. Prior to the preparation of hGal-1 samples for spectroscopic examination, the protein was incubated in aqueous 8 mM β-ME (pH 8.2) or 2 mM tris(2-carboxyethyl)-phosphine (TCEP, HCl salt) for 3 h at 37 °C to ensure the absence of the oxidized form that is inactive in galactoside binding.[30] TCEP was used to minimize the interfering UV absorption from the reducing reagent. The concentration of hGal-1 was determined in dimer units using the molar

extinction coefficient (16960 M^{-1} cm^{-1} at 280 nm) calculated from the numbers of Trp and Tyr residues in the protein.[31]

Aqueous samples of hGal-1 for UV absorption measurements were prepared at a concentration of 15.3 μM (0.45 mg/mL). The pH of the acidic solution of hGal-1 containing 2 mM TCEP was adjusted by adding aliquots of concentrated NaOH. CD and fluorescence spectra were measured for solutions containing 5.1 μM (0.15 mg/mL) hGal-1 dissolved in 20 mM citrate (pH 4−6), phosphate (pH 6−8), or Tris buffer (pH >8) supplemented with 20 mM NaCl and 4 mM β-ME. Samples for Raman spectroscopic measurements were prepared by using D_2O instead of H_2O to monitor the Raman bands of N-deuterated His residues. The exchange of labile protons with deuterons was ensured by a 3 h incubation of the protein in D_2O followed by lyophilization. The predeuterated sample of hGal-1 was dissolved at a concentration of 34 μM (1 mg/mL) in D_2O buffer supplemented with 20 mM NaCl and 4 mM β-ME. A 20 mM mixture of piperazine-1,4-bis(propanesulfonic acid) and 2-(*N*-morpholino)ethanesulfonic acid was used as the buffer to avoid overlap of the His and buffer Raman bands. $NaNO_3$ was added at a concentration of 2 mM, and the 1047 cm^{-1} Raman band of NO_3^- was used as an internal intensity standard.

Lactose was purchased from Nacalai Tesque and used without further purification. The concentration of lactose was determined by weight.

Acquisition of Spectra. UV absorption spectra were recorded on a Hitachi U-3310 spectrometer using a 1 mm cell and a spectral slit width of 5 nm. A JASCO J-820 spectropolarimeter was used to measure CD spectra with a 1 mm cell and a 2 nm spectral slit width. Fluorescence spectra were recorded on a JASCO FP-6500 spectrofluorometer with a spectral slit width of 5 nm for both excitation and emission. The fluorescence excitation wavelength was set at 295 nm to maximize the emission around 345 nm from the unique Trp (Trp68) and to minimize that from two Tyr residues (Tyr104 and Tyr119) in a shorter wavelength region. UV Raman scattering was excited at 229 nm by using a frequency-doubled Ar^+ laser (Innova 300 FReD, Coherent). The scattered Raman light was dispersed and detected on a UV Raman spectrometer (TR-600UV, JASCO) equipped with a liquid nitrogen-cooled CCD detector (LN/CCD-1152, Princeton Instruments). Raman spectral signals were accumulated for 320 s per spectrum, and four spectra of fresh samples were averaged. Wavenumber calibration of Raman spectra was effected by using a 1:1 mixture of cyclohexanone and acetonitrile. The peak positions of sharp Raman bands were reproducible within ±1 cm^{-1}.

Equilibrium Analysis of Lactose−hGal-1 Binding. Dimeric hGal-1 has two CRDs and can bind up to two lactose molecules. The binding may occur in the two following steps:

$$\text{hGal-1} + 2\text{Lac} \leftrightarrow \text{hGal-1}{-}\text{Lac} + \text{Lac} \leftrightarrow \text{hGal-1}{-}\text{Lac}_2 \quad (1)$$

In this study, however, hGal-1−Lac and hGal-1−Lac_2 could not be distinguished from each other by fluorescence spectroscopy (see below), and therefore, we analyzed the reaction by using the one-step binding model (eq 2), which takes into account the cooperativity of the lactose binding to the two CRDs using the Hill coefficient *n*.[33]

$$\text{hGal-1} + n\text{Lac} \leftrightarrow \text{hGal-1}{-}\text{Lac}_n \quad (2)$$

where *n* is larger or smaller than unity when the lactose binding to the hGal-1 dimer is positively or negatively cooperative, respectively. According to this one-step binding model, the apparent binding constant K_b is defined as follows.

$$K_b = [\text{hGal-1}{-}\text{Lac}_n]/[\text{hGal-1}][\text{Lac}]^n \quad (3)$$

The values of K_b and *n* were obtained from fluorescence spectra by using a combination of singular-value decomposition (SVD) and ordinary equilibrium analysis.[32−34] First, a set of fluorescence spectra were observed at a given pH for 5.1 μM hGal-1 in the presence of 17 different lactose concentrations. Then the set of spectra was analyzed by SVD to find the number and shapes of significant spectral components (basis spectra) required to reproduce the experimental spectra.[32,33] The SVD analysis indicated the necessity and sufficiency of two basis spectra at every pH examined, being consistent with the binding model of eq 2 that involves two fluorescent species, namely lactose-free and lactose-bound hGal-1. The SVD analysis also gave two basis spectra, b_j (j = 1 or 2), and coefficients $c_{i,j}$ (i = 1−17, and j = 1 or 2) in eq 4 to approximate each experimental spectrum d_i (i = 1−17) as follows:

$$d_i = c_{i,1}b_1 + c_{i,2}b_2 \quad (4)$$

On the other hand, the spectra of two fluorescent components s_k (k = 1 and 2 for lactose-free and lactose-bound hGal-1, respectively) were assumed to be expressed as a linear combination of b_j using unknown coefficients $f_{k,j}$:

$$s_k = f_{k,1}b_1 + f_{k,2}b_2 \quad (5)$$

By using s_k's and the concentrations of lactose-free hGal-1 ($[\text{hGal-1}]_i$) and lactose-bound hGal-1 ($[\text{hGal-1}{-}\text{Lac}_n]_i$) in the sample of the *i*th spectrum, the experimental spectrum d_i was also expressed as follows:

$$d_i = [\text{hGal-1}]_i s_1 + [\text{hGal-1}{-}\text{Lac}_n]_i s_2 \quad (6)$$

Substitution of eq 5 into eq 6 and comparison of the resultant equation with eq 4 yield the following equation:

$$c_{i,j} = [\text{hGal-1}]_i f_{1,j} + [\text{hGal-1}{-}\text{Lac}_n]_i f_{2,j} \quad (7)$$

With the total concentration of hGal-1 (in this study, 5.1 μM for every sample) denoted by g_0, eq 7 is rewritten as follows:

$$c_{i,j} = [\text{hGal-1}]_i (f_{1,j} - f_{2,j}) + g_0 f_{2,j} \quad (8)$$

In the actual SVD-based equilibrium analysis,[34] the value of $c_{i,j}$ (i = 1−17, and j = 1 or 2) on the left side of eq 8 was obtained by SVD analysis of the 17 experimental spectra. The values of $f_{1,j}$ and $f_{2,j}$ (j = 1 or 2) on the right side of eq 8 were regarded as unknown parameters, and $[\text{hGal-1}]_i$ (i = 1−17) was calculated from g_0 and the total concentration of lactose in the *i*th sample by using arbitrary initial values of K_b and *n* in eq 3. Refinement of the K_b and *n* values was achieved by least-squares calculations to reproduce $c_{i,j}$'s from the right side of eq 8. The most probable values of K_b, *n*, and $f_{k,j}$'s were thus determined from the experimentally obtained $c_{i,j}$'s. The spectra of lactose-free (s_1) and lactose-bound hGal-1 (s_2) were calculated from $f_{k,j}$'s using eq 5.

RESULTS

Lactose Binding Constant and Its pH Dependence. Figure 1a shows the fluorescence spectra of wild-type hGal-1 (5.1 μM) recorded at pH 7.5 and room temperature (~24 °C)

dx.doi.org/10.1021/bi4001112 | *Biochemistry* 2013, 52, 2371−2380

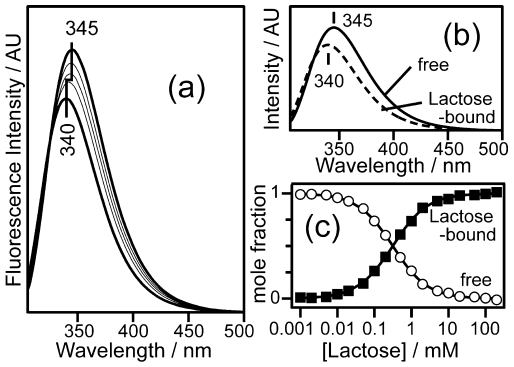

Figure 1. (a) Fluorescence spectra of wild-type hGal-1 (5.1 μM) at pH 7.4 (20 mM phosphate buffer) in the presence of 17 different lactose concentrations (0.001−200 mM). The fluorescence was excited at 295 nm. (b) Calculated fluorescence spectra for free (—) and lactose-bound (---) forms. The spectra were extracted from the experimental spectra in panel a by SVD-based equilibrium analysis. (c) Mole fractions of the free (○) and lactose-bound (■) forms of hGal-1 obtained by the SVD-based equilibrium analysis of the experimental spectra. The data are plotted vs the logarithmic concentration of lactose. The curves show theoretical mole fractions calculated from the equilibrium equation (eq 2) using the values of K_b and n determined by the same equilibrium analysis.

in the presence of 17 different lactose concentrations (0.001−200 mM). The fluorescence band peaking around 345 nm is ascribed to Trp68, which is the unique Trp residue in the subunit of hGal-1 and is one of the residues that compose the galactoside-binding pocket.[14] With the increase in the lactose concentration, the fluorescence band becomes weaker and shifts toward 340 nm. Because the peak wavelength of Trp fluorescence is known to decrease with an increase in the environmental polarity of the side chain indole ring,[35] the blue shift observed in Figure 1a indicates a decrease in the environmental polarity of Trp68 as a result of interaction with the bound lactose molecule. The weakening of fluorescence in Figure 1a may also be ascribed to the interaction with lactose. Thus, the fluorescence spectrum of Trp68 can be used as a probe for the binding of lactose to hGal-1.

By applying the SVD-based equilibrium analysis method described in Materials and Methods, we determined the binding constant K_b and the Hill coefficient n of lactose−hGal-1 binding (eq 3) from the fluorescence spectra depicted in Figure 1a. At pH 7.4, ~24 °C, and 20 mM NaCl, the K_b value was determined to be 2.94 ± 0.10 mM^{-1}, which is between two K_b values reported previously by using isothermal titration calorimetry: 3.25 ± 0.15 mM^{-1} (pH 7.2, 25 °C, and 200 mM NaCl)[14] and 2.44 ± 0.03 mM^{-1} (pH 7.4, 30 °C, and no NaCl).[36] If we take into account the differences in pH, temperature, and NaCl concentration, the K_b values obtained here are in reasonable agreement with the literature values, giving support to the reliability of our equilibrium analysis method.

The Hill coefficient n determined by the SVD-based equilibrium analysis is 0.93 ± 0.02, which suggests a weak negative cooperativity of for binding of lactose to the hGal-1 dimer. A previous calorimetric titration based on a sequential binding model involving lactose-free, half-bound, and fully bound hGal-1 dimers showed that the first binding is stronger than the second, being consistent with the negative cooperativity observed here.[36] Although we also attempted to fit the experimental fluorescence spectra to the sequential binding model of eq 1, the experimental spectra were not so well reproduced as in the one-step binding model of eq 2. Probably, the intersubunit interaction responsible for the negative cooperativity is not so strong that it influences the fluorescence spectrum of Trp68, and the half-bound and fully bound dimers cannot be distinguished from each other by fluorescence spectroscopy. Actually, SVD analysis has shown that two spectral components (corresponding to the lactose-free and lactose-bound states) are sufficient for reproducing the fluorescence spectra of lactose−hGal-1 mixtures (see Materials and Methods).

Figure 1b shows the fluorescence spectra of lactose-free and lactose-bound hGal-1 obtained via SVD-based equilibrium analysis. The peak positions of the spectra are 345 nm (lactose-free) and 340 nm (lactose-bound), which are in agreement with those observed in the presence of 0.001 and 200 mM lactose, respectively (Figure 1a). The mole fractions of lactose-free and lactose-bound hGal-1 can be derived from the experimental fluorescence spectra by using eq 6, and they are plotted against the concentration of lactose (on a log scale) in Figure 1c. Also shown are the curves of mole fractions calculated from K_b and n by using eq 3. The calculated curves closely trace the plots of experimental mole fractions, demonstrating the self-consistency of the SVD-based equilibrium analysis.

The SVD-based equilibrium analysis was also applied to the fluorescence spectra recorded at pH 4.0−9.0 to determine the K_b values. Figure 2 shows the plot of K_b of wild-type hGal-1

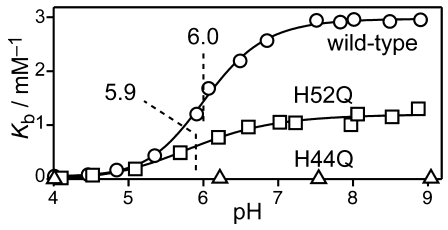

Figure 2. pH dependence of lactose binding constant K_b for wild-type hGal-1 (○), H44Q (△), and H52Q (□). The K_b values at individual pH values were determined in the same way as shown for pH 7.4 in Figure 1. The curves represent fits with sigmoidal functions.

versus pH (○). The value of K_b is nearly constant above pH 7.5, while it decreases below pH 7, being consistent with the pH dependence of galactoside binding activity reported in the literature.[18,19] The midpoint of the K_b change is seen at pH 6.0 ± 0.1. (The midpoint was determined by fitting the data points of K_b to a sigmoidal curve[37] as shown in Figure 2.) Analogous pH titration was also conducted for the H44Q and H52Q mutants. The K_b value obtained for the H44Q mutant is <0.02 mM^{-1} throughout the pH range examined [Figure 2 (△)]. This observation is consistent with the previous report that the H44Q mutant lost its galactoside binding activity,[15] suggesting a critical role of His44 in galactoside binding. The H52Q mutant, on the other hand, partially retains affinity for lactose [Figure 2 (□)]. The decreased affinity of H52Q indicates a contribution of His52 to the galactoside binding activity. The slight difference in the transition pH between H52Q (5.9 ± 0.1) and the wild type (6.0 ± 0.1) may also reflect the contribution of His52. The H52Q mutant contains only one His residue (His44), and therefore, it is likely that the pH dependence of this mutant reflects the protonation of the remaining His44 residue, whose pK_a is 5.9. On the other hand,

dx.doi.org/10.1021/bi4001112 | *Biochemistry* 2013, 52, 2371−2380

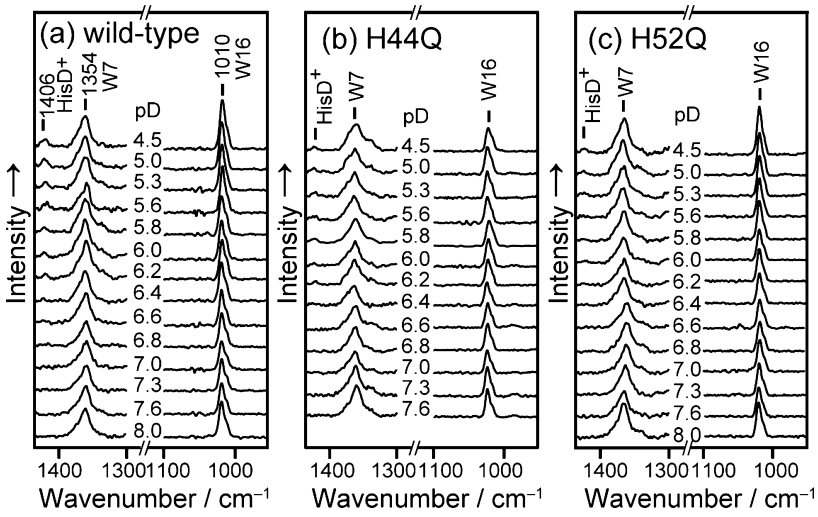

Figure 3. pD dependence of UV (229 nm) Raman spectra of (a) wild-type hGal-1, (b) H44Q, and (c) H52Q. The intensity in the 1300−1420 cm^{-1} region is magnified twice compared to that in the 1100−950 cm^{-1} region.

the apparent transition at pH 6.0 of wild-type hGal-1 may be explained by an overlapping effect of the protonation of His44 and His52, the pK_a of His52 being greater than that of His44.

pK_a Values of His Residues. To determine the pK_a values of His44 and His52 by a direct method, we measured UV (229 nm) Raman spectra of hGal-1 in a D_2O solution at varied pD values because Raman spectra in a D_2O solution provide Raman bands characteristic of the protonated form of His ($HisD^+$).[38,39] The UV Raman spectra recorded at pD 4.5−8.0 are shown in panels a−c of Figure 3 for the wild type, H44Q, and H52Q, respectively. The intensity scale is magnified twice in the 1420−1300 cm^{-1} region compared to that in the 1100−950 cm^{-1} region for better recognition of a weak band at 1406 cm^{-1} arising from $HisD^+$. It is evident that the intensity of the $HisD^+$ band increases with a decrease in pD.

The left panel of Figure 4 exhibits the pD dependence of the intensity of the $HisD^+$ band (I_{HisD^+}) measured relative to the 1047 cm^{-1} band of NO_3^- added as an internal intensity standard (not shown in the spectra in Figure 3). The transition midpoint of I_{HisD^+} is seen at pD 6.3 ± 0.1 for H44Q and at pD 5.7 ± 0.2 for H52Q. Because the transition pD of a mutant must correspond to the pK_a of the His residue remaining in the mutant, the pK_a values of His44 and His52 are thought to be 5.7 ± 0.2 and 6.3 ± 0.1, respectively. The average of pK_a's of these His residues is close to the apparent pK_a (6.0 ± 0.1) observed for wild-type hGal-1 containing both His44 and His52. The transition pH of the lactose binding constant (K_b) observed for the H52Q mutant [5.9 ± 0.1 (Figure 2)] is in agreement with the pK_a of His44 (5.7 ± 0.2) within experimental error. Furthermore, the transition midpoint pH of K_b observed for the wild type [6.0 ± 0.1 (Figure 2)] is between the pK_a values of His44 (5.7 ± 0.2) and His52 (6.3 ± 0.1). The coincidence between the transition pH of K_b and the His pK_a strongly suggests a close link between the decrease in the lactose binding activity at acidic pH and the protonation of His44 and His52.

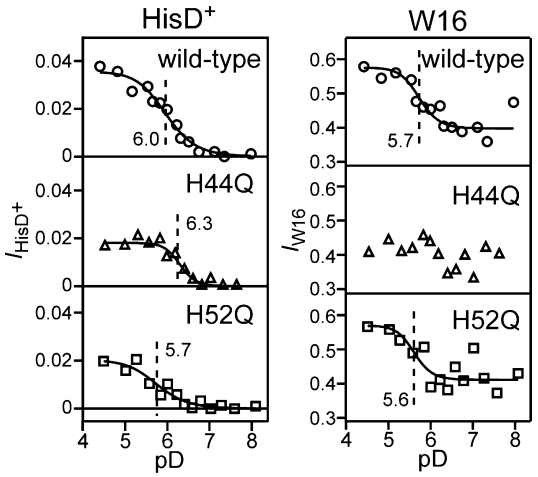

Figure 4. pD dependence of the $HisD^+$ (left) and Trp W16 (right) Raman band intensities for wild-type hGal-1 (top), H44Q (middle), and H52Q (bottom). The integrated intensities are evaluated from the spectra in Figure 3 and then normalized to the 1047 cm^{-1} band of NO_3^- (not shown in Figure 3) added as an internal intensity standard. The curves show fitting to the Hill equation.

Interaction of Trp68 with His44 and the Environment. The UV Raman spectra in Figure 3 provide information about the structure and environment of Trp68 as well. The Raman band at 1010 cm^{-1} is assigned to the W16 vibration of the Trp indole ring,[40] and its UV Raman intensity is known to be sensitive to the indole ring environment and hydrogen bonding.[41] The intensity of the W16 Raman band is plotted against pD in the right panel of Figure 4. The W16 intensity increases at acidic pD in wild-type hGal-1 and in the H52Q mutant with a transition at nearly identical pD values (5.7 ± 0.2 for the wild type and 5.6 ± 0.2 for H52Q). In contrast, no systematic change in W16 intensity is seen for the H44Q mutant. These observations clearly indicate that the W16 band is intensified by the protonation of His44 but not by the protonation of His52. The interaction of Trp68 with only His44 is consistent with the X-ray structure of hGal-1, in which Trp68 is in the proximity of His44 but far from His52.[14]

A broad Raman band around 1350 cm^{-1} in Figure 3 is ascribed to the W7 doublet.[42] The intensity ratio of the doublet components at 1360 and 1340 cm^{-1} is known to serve as a marker of the hydrophobic interaction of Trp with the surroundings:[40,43] the stronger the hydrophobic interaction, the higher the intensity ratio (I_{1360}/I_{1340}). Unfortunately, however, the buffer used here gave strong Raman bands in

dx.doi.org/10.1021/bi4001112 | Biochemistry 2013, 52, 2371−2380

the wavenumber region of W7, and reliable evaluation of the W7 doublet intensity ratio could not be made.

Fluorescence spectroscopy was also utilized to investigate the pH dependence of the Trp68 environment (Figure 5). Wild-

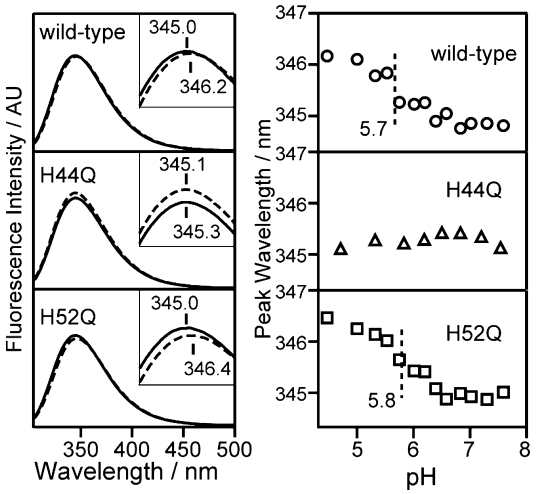

Figure 5. Fluorescence spectra (left) of wild-type hGal-1 (top), H44Q (middle), and H52Q (bottom) at pH 7 (—) and 5 (---). The excitation wavelength is 295 nm. The inset shows magnified traces in the 330−360 nm region. pH dependence (right) of the fluorescence peak wavelength for wild-type hGal-1 (top), H44Q (middle), and H52Q (bottom).

type hGal-1 exhibits a red shift of the peak wavelength of Trp fluorescence from 345.0 to 346.2 nm at pH 5.7 ± 0.3 [Figure 5, right panel (○)], and the H52Q mutant also exhibits a comparable red shift at pH 5.8 ± 0.1 [Figure 5, right panel (□)]. These transition pH values are again in agreement with the pK_a of His44 (5.7 ± 0.2) within experimental error, giving support to the presence of an interaction between Trp68 and His44. The interaction between Trp68 and His44 is consistent with the lack of a peak shift in Trp fluorescence in the H44Q mutant [Figure 5, right panel (△)]. Because a red shift of Trp fluorescence is a marker of the increase in the polarity of the Trp environment,[35] the fluorescence spectra of hGal-1 in Figure 5 indicate that the environment of Trp68 becomes more polar upon protonation of His44.

The interaction between Trp68 and His44 is also supported by UV absorption spectroscopy. Figure 6a compares the UV absorption spectra of wild-type hGal-1 at pH 7.5 and 4.5. Although the effect of the change in pH is not apparent in the

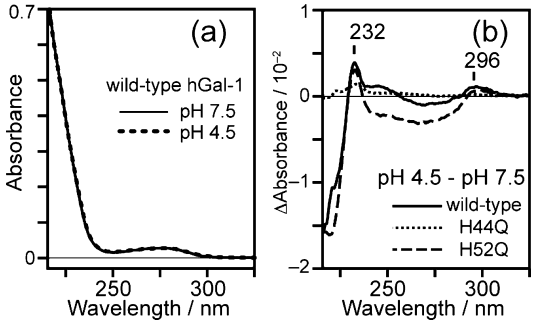

Figure 6. (a) UV absorption spectra of wild-type hGal-1 at pH 4.5 (—) and 7.5 (···). (b) Difference in UV absorption (pH 4.5 minus pH 7.5) for wild-type hGal-1 (—), H44Q (···), and H52Q (---).

spectra of Figure 6a, the difference spectrum (pH 4.5 minus pH 7.5) in Figure 6b reveals small but significant changes associated with the acidification. The negative feature below 227 nm and the positive peak at 232 nm in the difference spectrum (Figure 6b, solid line) can be explained by assuming a red shift of the Trp B_b absorption band around 220 nm accompanied by an intensity decrease. A weakening of amide UV absorption of the peptide main chain may also contribute to the negative difference features below 220 nm. The features in the difference spectrum remain in the H52Q mutant but disappear in the H44Q mutant. An analogues change in the B_b absorption band has been reported for cation−π interactions involving the indole ring of Trp or its analogue,[39,44,45] and therefore, the UV absorption change in Figure 6 is ascribed to a cation−π interaction between the protonated His44 and Trp68. The occurrence of the cation−π interaction is consistent with the increase in the environmental polarity of Trp68 detected as a red shift of fluorescence upon protonation of His44 (Figure 5).

The increase in absorption intensity at 229 nm observed for the wild type and H52Q (Figure 6b, solid and dotted lines) is expected to induce an enhancement of B_b-resonant Raman bands, including the W16 band.[39] Actually, the intensity of the W16 Raman band of hGal-1 recorded with 229 nm excitation increases upon protonation of His44 as described above. On the other hand, a weak positive peak at 296 nm in the difference absorption spectrum of wild-type hGal-1 is attributed to a red shift of the L_a absorption band, which may also be caused by the cation−π interaction.[39,44,45] Although the hyperchromicity at 296 nm at acidic pH is expected to intensify the Trp68 fluorescence by increasing the absorption of excitation light at 295 nm, the fluorescence intensity does not largely change between pH 5.0 and 7.0 for the wild type or mutants (Figure 5, left panel). Probably, the increased excitation efficiency is offset by a quenching of the fluorescence emission by the positively charged imidazole ring of His44.[46]

pH Dependence of Secondary Structure. CD spectroscopy is a tool for analyzing the main chain conformation of proteins. In the CD spectrum of wild-type hGal-1 (Figure 7, left

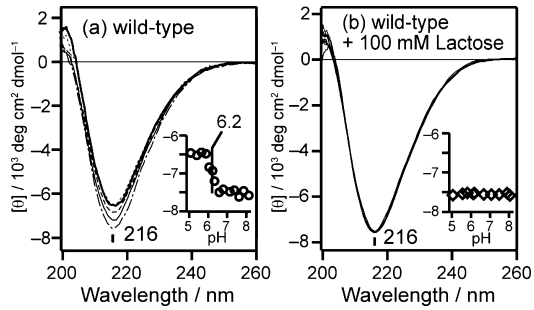

Figure 7. CD spectra of wild-type hGal-1 at pH 5.5 (thick solid line), 5.9 (···), 6.0 (---), 6.3 (thin solid line), and 8.0 (·—·) in the (a) absence and (b) presence of lactose (100 mM). The molar ellipticity [θ] at 216 nm is plotted vs pH in the inset.

panel), a negative peak appears at 216 nm, which is ascribed to 11 β-strands comprising the jellyroll structure of hGal-1.[14] With a decrease in pH from neutral to acidic, the peak intensity of the 216 nm negative band shows a weakening at pH 6.2 ± 0.1 (Figure 7, left panel, inset). In contrast, the peak wavelength does not deviate from 216 nm at any pH, implying the absence of a large change in secondary structure. The reduced intensity

dx.doi.org/10.1021/bi4001112 | Biochemistry 2013, 52, 2371−2380

of the 216 nm band below pH 6.2 may be ascribed to a partial rearrangement or unfolding of β-strands within the jellyroll structure of hGal-1. Because the transition pH observed in the CD spectra (6.2 ± 0.1) is in agreement with the pK_a of His52 (6.3 ± 0.1) derived from Raman spectra (Figure 4), the secondary structure seems to be affected, possibly very locally, by the protonation and/or deprotonation of His52. In the presence of 100 mM lactose that fills the galactoside-binding pocket of hGal-1, the CD spectrum is not affected by pH (Figure 7, right panel), suggesting that the partial change in secondary structure occurs within or beside the galactoside-binding pocket.

DISCUSSION

Structural Change and His Protonation. Table 1 summarizes the midpoint pH values of the structural changes in hGal-1 observed in Raman, CD, and fluorescence spectra. Because H44Q and H52Q mutants contain only one His residue, analysis of the $HisD^+$ Raman band intensity straightforwardly gives the pK_a value of the His residue remaining in each mutant (His52 in H44Q and His44 in H52Q) (Figure 4). The obtained pK_a value is 5.7 ± 0.2 for His44 and 6.3 ± 0.1 for His52 as shown in the top row of Table 1. The Trp W16 Raman band intensity (Figure 4) and the Trp fluorescence peak wavelength (Figure 5) have indicated an environmental change in Trp68 at pH 5.6 ± 0.2 and 5.8 ± 0.1, respectively. These pH values are substantially the same as the pK_a of His44, and therefore, the environmental change of Trp68 in H52Q is ascribed to the protonation of His44. The change in lactose binding activity observed at pH 5.9 ± 0.1 for H52Q (Figure 2) can also be attributed to the protonation of His44.

Table 1. Midpoint pH Values of the Structural Changes of hGal-1 Observed in Raman, CD, and Fluorescence Spectra

method	observed change	wild type (H44 and H52)[a]	H44Q (H52)[a]	H52Q (H44)[a]
Raman	protonation of His	6.0 ± 0.1 (H44, H52)[b]	6.3 ± 0.1	5.7 ± 0.2
Raman	Trp environmental change	5.7 ± 0.2 (H44)[b]	–	5.6 ± 0.2
CD	secondary structure change	6.2 ± 0.1 (H52)[b]	–	–
fluorescence	Trp environmental change	5.7 ± 0.3 (H44)[b]	–	5.8 ± 0.1
fluorescence	lactose affinity change	6.0 ± 0.1 (H44, H52)[b]	–	5.9 ± 0.1

[a]His residue(s) contained in the protein. [b]His residue(s) contributing to the observed change of wild-type hGal-1. For mutants H44Q and H52Q, all spectral changes are assigned to the remaining unique His residue.

For wild-type hGal-1, which contains both His44 and His52, the pK_a of His protonation and the pK_b of lactose binding are close to the average (6.0) of the pK_a values of His44 and His52 (top and bottom rows in Table 1), suggesting contributions of both His residues. Analogously, comparison of the midpoint pH of spectral change with the pK_a values of His44 and His52 indicates that the environmental change of Trp in wild-type hGal-1 detected by Raman and fluorescence spectroscopy is ascribed to the protonation of His44 (second and fourth rows in Table 1), while the secondary structure change detected by CD spectroscopy is attributed to His52 protonation (third row in Table 1). The data in Table 1 clearly show that the protonation of His44 affects the environment of Trp68 and the lactose binding activity. On the other hand, the protonation of His52 induces a change in secondary structure and in lactose binding activity.

Structural Mechanism of the pH Dependence of Lactose Binding Activity. To understand the mechanism of the pH dependence of lactose binding activity in terms of the pH-dependent structural changes revealed in this study (Table 1), we examined eight structures of hGal-1 deposited in the Protein Data Bank (PDB).[14,27,36] Among them, we chose two X-ray crystal structures as models of the lactose-bound and lactose-free forms of hGal-1. The lactose-bound model was taken from the structure at pH 7.0 of a mutant of hGal-1 (chain A) having all six Cys residues replaced with Ser (PDB entry 2ZKN).[27] On the other hand, the structure at pH 5.6 of the Cys2 → Ser mutant of hGal-1 (chain B) was employed as the model of the lactose-free form (PDB entry 1W6N).[14] Figure 8 compares the two models; the lactose-free form is colored orange.

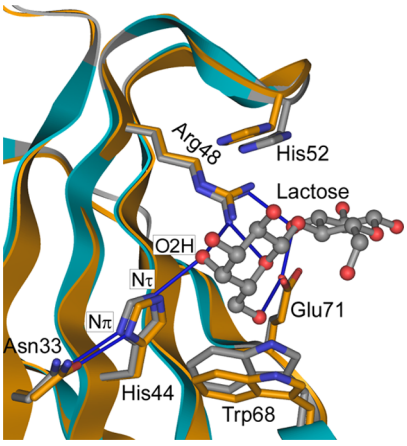

Figure 8. Comparison of the structures of lactose-bound (pH 7.0) and lactose-free (pH 5.6) hGal-1. The lactose-free form is colored orange. Blue lines represent hydrogen bonds. The atomic coordinates were taken from PDB entries 2ZKN[27] and 1W6N.[14]

In the lactose-bound form at neutral pH, four OH groups of lactose are involved in six hydrogen bonds with His44, Arg48, and Glu71. In the hydrogen bond between O2H of the galactose moiety of lactose and the Nτ site of His44, the Nτ atom accepts a hydrogen atom from O2H because the guanidinium group of Arg48 supplies O2H with another hydrogen atom. The original hydrogen atom at the Nπ site of His44 is used to form a hydrogen bond with the C═O group of the Asn33 side chain. In the other four hydrogen bonds involving lactose, lactose acts as the acceptor of a hydrogen from Arg48 or as a donor of a hydrogen to Glu71. In addition to the hydrogen bonds, the lactose molecule is sandwiched at the center of the binding pocket by the imidazole ring of His52 and the indole ring of Trp68.

His52 and His44 undergo protonation at pH 6.3 and 5.7, respectively (Table 1). The lactose-free form at acidic pH depicted in Figure 8 suggests that protonated His52 moves away from Arg48, probably because of electrostatic repulsion between the cationic imidazole ring of His52 and the cationic guanidinium side chain of Arg48. The movement of His52 is

dx.doi.org/10.1021/bi4001112 | Biochemistry 2013, 52, 2371−2380

accompanied by a partial unfolding of the β-strand containing His52 and a widening of the mouse of the lactose binding pocket, being consistent with the secondary structural change detected at pH 6.3 by CD spectroscopy (Table 1). The protonation of His44, on the other hand, produces more pronounced structural effects. First, His44 is no longer able to form a hydrogen bond with lactose as a proton acceptor because Nτ is already protonated by solvent water in the cationic state of His44. In addition to the lack of hydrogen bonding interaction, a reorientation or displacement of the Trp68 indole is induced by the cation−π interaction between His44 and Trp68. The movement of Trp68 loosens the lactose-binding pocket and reduces the force to retain the lactose molecule at the center of the binding pocket. The structural changes associated with the protonation of His52 and His44 are all unfavorable for lactose binding and may explain the reduction in the lactose binding activity of hGal-1 at acidic pH.

Biological Implication of the pH Dependence of Lactose Binding Activity. Metastasis of cancer cells at the culmination of neoplastic progression is initiated by liberation of cancer cells from the primary lesion.[47,48] Extracellular matrix (ECM) serves as a scaffold that provides structural support for cells and cancer cells in tissue, and the liberation of cancer cells involves degradation of ECM[49] by proteases activated in an acidic microenvironment of the cancer cell surface (pH ∼5.5).[20−22] The low extracellular pH is a consequence of the high metabolic activity of hypoxic cancer cells proliferating in solid tumor because the hypoxic cells perform anaerobic glycolysis and transport lactic acid, a product of the anaerobic glycolysis, to the extracellular space.[50] hGal-1 mediates adhesion between ECM and cells by linking ECM to cell surface β-galactoside, including that of cancer cells.[5,8,12,51−56] Therefore, it is possible that hGal-1 is also involved in the facilitation of metastasis because the galactoside binding activity of hGal-1 would be diminished at the acidified cancer cell surface (Figure 2), inducing detachment of the cancer cell from ECM.

Another example of the biological implication of hGal-1 may be found in endocytosis, a mechanism by which cells take in extracellular materials. The extracellular material is endocytosed after binding to receptors on the cell membrane surface. The cell membrane invaginates to form a vesicle termed an endosome, and the material bound to the receptor is wrapped in the endosome and internalized in the cell. Subsequent acidification of the endosomal compartment induces detachment of the bound material from the receptor, followed by degradation of the released material.[57,58] In leukemic T cells, the endocytosis of hGal-1 is mediated by ganglioside GM1,[59] a ubiquitous cell surface glycolipid and a receptor for hGal-1.[52] A membrane glycoprotein CD7 travels with the complex of hGal-1 and GM1 as a bystander (that is, CD7 does not take part in the endocytosis of hGal-1 because the hGal-1 internalization also occurs in a CD7 deficient T cell line).[59] CD7 is a membrane glycoprotein with two N-linked glycans[60] and is another receptor for hGal-1 that transmits the apoptotic signal of hGal-1 in T cells.[61] The β-galactoside binding activity of hGal-1 at neutral pH may help the formation of a ternary complex of hGal-1 with GM1 and CD7 in the extracellular space, and the decrease in the β-galactoside binding affinity at acidic pH would facilitate the destruction of the ternary complex in the endosomal compartment for subsequent degradation.[59]

CONCLUSION

We have investigated the structural basis of the reduction of the galactoside binding activity of hGal-1 at acidic pH by examining fluorescence, CD, and UV Raman spectra of wild-type hGal-1 and its H44Q and H52Q mutants at varied pH values in the absence and presence of lactose. Analysis of the spectral data with reference to literature X-ray structures of hGal-1 has suggested that the protonation of His52 below pH 6.3 induces a slight movement of His52 away from the galactoside-binding region accompanied by a partial unfolding of the β-strand containing His52. On the other hand, the protonation of His44 below pH 5.7 makes this residue unable to form a hydrogen bond with galactoside and additionally induces a reorientation and/or displacement of Trp68 through cation−π interaction, resulting in a loosened galactoside-binding pocket. These structural changes induced by His protonation are likely to be the origin of the pH dependence of the galactoside binding activity of hGal-1.

AUTHOR INFORMATION

Corresponding Author

*Phone: +81-22-795-6856. Fax: +81-22-795-6854. E-mail: hiramatu@m.tohoku.ac.jp.

Funding

This work was supported by a Grant-in-Aid for Scientific Research (B) (23390008) and a Grant-in-Aid for Young Scientists (B) (24790039) from Japan Society for the Promotion of Science.

Notes

The authors declare no competing financial interest.

ABBREVIATIONS

CD, circular dichroism; CRD, carbohydrate recognition domain; hGal-1, human galectin-1; H44Q, His44 → Gln mutant of hGal-1; H52Q, His52 → Gln mutant of hGal-1; K_b, lactose binding constant; PDB, Protein Data Bank; SVD, singular-value decomposition; TCEP, tris(2-carboxyethyl)-phosphine; UV, ultraviolet.

REFERENCES

(1) Barondes, S. H., Castronovo, V., Cooper, D. N. W., Cummings, R. D., Drickamer, K., Felzi, T., Gitt, M. A., Hirabayashi, J., Hughes, C., Kasai, K., Leffler, H., Liu, F. T., Lotan, R., Mercurio, A. M., Monsigny, M., Pillai, S., Polrer, F., Raz, A., Rigby, P. W. J., Rini, J. M., and Wang, J. L. (1994) Galectins: A family of animal β-galactoside-binding lectins. *Cell 76*, 597−598.

(2) Barondes, S. H., Cooper, D. N. W., Gitt, M. A., and Leffler, H. (1994) Galectins: Structure and function of a large family of animal lectins. *J. Biol. Chem. 269*, 20807−20810.

(3) Rabinovich, G. A., Baum, L. G., Tinari, N., Paganelli, R., Natoli, C., Liu, F. T., and Iacobelli, S. (2002) Galectins and their ligands: Amplifiers, silencers or tuners of the inflammatory response? *Trends Immunol. 23*, 313−320.

(4) Yang, R.-Y., Rabinovich, G. A., and Liu, F. T. (2008) Galectins: Structure, function and therapeutic potential. *Expert Rev. Mol. Med. 10*, e17.

(5) Camby, I., Le Mercier, M., Lefranc, F., and Kiss, R. (2006) Galectin-1: A small protein with major functions. *Glycobiology 16*, 137R−157R.

(6) Giudicelli, V., Lutomski, D., Lévi-Strauss, M., Bladier, D., Joubert-Caron, R., and Caron, M. (1997) Is human galectin-1 activity modulated by monomer/dimer equilibrium? *Glycobiology 7*, viii−x.

(7) Perillo, N. L., Marcus, M. E., and Baum, L. G. (1998) Galectins: Versatile modulators of cell adhesion, cell proliferation, and cell death. *J. Mol. Med. 76*, 402−412.
(8) Huges, R. C. (2001) Galectins as modulators of cell adhesion. *Biochimie 83*, 667−676.
(9) van den Brule, F., Califice, S., and Castronovo, V. (2004) Expression of galectins in cancer: A critical review. *Glycoconjugate J. 19*, 537−542.
(10) Brewer, C. F. (2002) Binding and cross-linking properties of galectins. *Biochim. Biophys. Acta 1572*, 255−262.
(11) Scott, K., and Weinberg, C. (2002) Galectin-1: A bifunctional regulator of cellular proliferation. *Glycoconjugate J. 19*, 467−477.
(12) Rabinovich, G. A. (2005) Galectin-1 as a potential cancer target. *Br. J. Cancer 92*, 1188−1192.
(13) Hirabayashi, J., and Kasai, K. (1988) Complete amino acid sequence of a β-galactoside-binding lectin from human placenta. *J. Biochem. 104*, 1−4.
(14) López-Lucendo, M. F., Solís, D., André, S., Hirabayashi, J., Kasai, K., Kaltner, H., Gabius, H.-J., and Romero, A. (2004) Growth-regulatory human galectin-1: Crystallographic characterisation of the structural changes induced by single-site mutations and their impact on the thermodynamics of ligand binding. *J. Mol. Biol. 343*, 957−970.
(15) Hirabayashi, J., and Kasai, K. (1994) Further evidence by site-directed mutagenesis that conserved hydrophilic residues form a carbohydrate-binding site of human galectin-1. *Glycoconjugate J. 11*, 437−442.
(16) Hirabayashi, J., and Kasai, K. (1991) Effect of amino acid substitution by site-directed mutagenesis on the carbohydrate recognition and stability of human 14-kDa β-galactoside-binding lectin. *J. Biol. Chem. 266*, 23648−23653.
(17) Grimsley, G. R., Scholtz, J. M., and Pace, C. N. (2009) A summery of the measured pK values of the ionizable groups in folded proteins. *Protein Sci. 18*, 247−251.
(18) Ahmed, H., Allen, H. J., Sharma, A., and Matta, K. L. (1990) Human spleen galaptin: Carbohydrate-binding specificity and characterization of the combining site. *Biochemistry 29*, 5315−5319.
(19) Lee, R. T., Ichikawa, Y., Allen, H. J., and Lee, Y. C. (1990) Binding characteristics of galactoside-binding lectin (galaptin) from human spleen. *J. Biol. Chem. 265*, 7864−7871.
(20) Thistlethwaite, A. J., Leeper, D. B., Moylan, D. J., III, and Nerlinger, R. E. (1985) pH distribution in human tumors. *Int. J. Radiat. Oncol., Biol., Phys. 11*, 1647−1652.
(21) Griffiths, J. R. (1991) Are cancer cells acidic? *Br. J. Cancer 64*, 425−427.
(22) Schaefer, C., Mayer, W.-K., Krüger, W., and Vaupel, P. (1993) Microregional distributions of glucose, lactate, ATP and tissue pH in experimental tumours upon local hypertheria and/or hyperglycaemia. *J. Cancer Res. Clin. Oncol. 119*, 599−608.
(23) Jacobus, W. E., Taylor, G. J. T., Hollis, D. P., and Nunnally, R. L. (1977) Phosphorus nuclear magnetic resonance of perfused working rat hearts. *Nature 265*, 756−758.
(24) Geborek, P., Saxne, T., Pettersson, H., and Wollheim, F. A. (1989) Synovial fluid acidosis correlates with radiological joint destruction in rheumatoid arthritis knee joints. *J. Rheumatol. 16*, 468−472.
(25) Ohkuma, S., and Poole, B. (1978) Fluorescence probe measurement of the intralysosomal pH in living cells and the perturbation of pH by various agents. *Proc. Natl. Acad. Sci. U.S.A. 75*, 3327−3331.
(26) Mellman, I., Fuchs, R., and Helenius, A. (1986) Acidification of the endocytic and exocytic pathways. *Annu. Rev. Biochem. 55*, 663−700.
(27) Nishi, N., Abe, A., Iwaki, J., Yoshida, H., Itoh, A., Shoji, H., Kamitori, S., Hirabayashi, J., and Nakamura, T. (2008) Functional and structural bases of a cysteine-less mutant as a long-lasting substitute for galectin-1. *Glycobiology 18*, 1065−1073.
(28) Hirabayashi, J., Ayaki, H., Soma, G., and Kasai, K. (1989) Cloning and nucleotide sequence of a full-length cDNA for human 14 kDa β-galactoside-binding lectin. *Biochim. Biophys. Acta 1008*, 85−91.
(29) Hirabayashi, J., Ayaki, H., Soma, G., and Kasai, K. (1989) Production and purification of a recombinant human 14 kDa β-galactoside-binding lectin. *FEBS Lett. 250*, 161−165.
(30) Inagaki, Y., Sohma, Y., Horie, H., Nozawa, R., and Kadoya, T. (2000) Oxidized galectin-1 promotes axonal regeneration in peripheral nerves but does not possess lectin properties. *Eur. J. Biochem. 267*, 2955−2964.
(31) Pace, C. N., Vajdos, F., Fee, L., Grimsley, G., and Gray, T. (1995) How to measure and predict the molar absorption coefficient of a protein. *Protein Sci. 4*, 2411−2423.
(32) Frans, S. D., and Harris, J. M. (1985) Least squares singular value decomposition for the resolution of pK's and spectra from organic acid/base mixtures. *Anal. Chem. 57*, 1718−1721.
(33) Hendler, R. W., and Shrager, R. I. (1994) Deconvolutions based on singular value decomposition and the pseudoinverse: A guide for beginners. *J. Biochem. Biophys. Methods 28*, 1−33.
(34) Asagi, M., Toyama, A., and Takeuchi, H. (2010) Binding affinity and mode of distamycin A with A/T stretches in double-stranded DNA: Importance of the terminal A/T residues. *Biophys. Chem. 149*, 34−39.
(35) Burstein, E. A., Vedenkina, N. S., and Ivkova, M. N. (1973) Fluorescence and the location of tryptophan residues in protein molecules. *Photochem. Photobiol. 18*, 263−279.
(36) Nesmelova, I. V., Ermakova, E., Daragan, V. A., Pang, M., Menéndez, M., Lagartera, L., Sólis, D., Baum, L. G., and Mayo, K. H. (2010) Lactose binding to galectin-1 modulates structural dynamics, increases conformational entropy, and occurs with apparent negative cooperativity. *J. Mol. Biol. 397*, 1209−1230.
(37) Cerny, L. C., Stasiw, D. M., and Zuk, W. (1981) The logistic curve for the fitting of sigmoidal data. *Physiol. Chem. Phys. 13*, 221−230.
(38) Chen, M. C., Lord, R. C., and Mendelsohn, R. (1973) Laser-excited Raman spectroscopy of biomolecules IV. Thermal denaturation of aqueous lysozyme. *Biochim. Biophys. Acta 328*, 252−260.
(39) Okada, A., Miura, T., and Takeuchi, H. (2001) Protonation of histidine and histidine-tryptophan interaction in the activation of the M2 ion channel from influenza A virus. *Biochemistry 40*, 6053−6060.
(40) Harada, I., and Takeuchi, H. (1986) Raman and ultraviolet resonance Raman spectra of proteins and related compounds. In *Spectroscopy of Biological Systems* (Clark, R. J. H., and Hester, R. E., Eds.) pp 113−175, John Wiley and Sons, New York.
(41) Matsuno, M., and Takeuchi, H. (1998) Effects of hydrogen bonding and hydrophobic interactions on the ultraviolet resonance Raman intensities of indole ring vibrations. *Bull. Chem. Soc. Jpn. 71*, 851−857.
(42) Harada, I., Miura, T., and Takeuchi, H. (1986) Origin of the doublet at 1360 and 1340 cm^{-1} in the Raman spectra of tryptophan and related compounds. *Spectrochim. Acta, Part A 42*, 307−312.
(43) Miura, T., Takeuchi, H., and Harada, I. (1988) Characterization of individual tryptophan side chains in proteins using Raman spectroscopy and hydrogen-deuterium exchange kinetics. *Biochemistry 27*, 88−94.
(44) Xue, Y., Davis, A. V., Balakrishnan, G., Stasser, J. P., Staehlin, B. M., Focia, B. M., Spiro, T. G., Penner-Hahn, J. E., and O'Halloran, T. V. (2008) Cu(I) recognition via cation-π and methionine interactions in CusF. *Nat. Chem. Biol. 4*, 107−109.
(45) Yorita, H., Otomo, K., Hiramatsu, H., Toyama, A., Miura, T., and Takeuchi, H. (2008) Evidence for the cation-π interaction between Cu^{2+} and tryptophan. *J. Am. Chem. Soc. 130*, 15266−15267.
(46) Chen, Y., and Barkley, M. D. (1998) Toward understanding tryptophan fluorescence in proteins. *Biochemistry 37*, 9976−9982.
(47) Hanahan, D., and Weinberg, R. A. (2000) The hallmarks of cancer. *Cell 100*, 57−70.
(48) Eccles, S. A., and Welch, D. R. (2007) Metastasis: Recent discoveries and novel treatment strategies. *Lancet 369*, 1742−1757.
(49) Koblinski, J. E., Ahram, M., and Sloane, B. F. (2000) Unraveling the role of proteases in cancer. *Clin. Chim. Acta 291*, 113−135.
(50) Dhup, S., Dadhich, R. K., Porporato, P. E., and Sonveaux, P. (2012) Multiple biological activities of lactic acid in cancer: Influence

on tumor growth, angiogenesis, and metastasis. *Curr. Pharm. Des. 18*, 1319−1330.
(51) Ranmkumar, R., and Podder, S. K. (2000) Elucidation of the mechanism of interaction of sheep spleen galectin-1 with splenocytes and its role in cell-matrix adhesion. *J. Mol. Recognit. 13*, 299−308.
(52) Elola, M. T., Chiesa, M. E., Alberti, A. F., Mordoh, J., and Fink, N. E. (2005) Galectin-1 receptors in different cell types. *J. Biomed. Sci. 12*, 13−29.
(53) Leffler, H. (1997) Introduction to galectins. *Trends Glycosci. Glycotechnol. 45*, 9−19.
(54) van den Brule, F. A., Buicu, C., Baldet, M., Sobel, M. E., Cooper, D. N. W., Marschal, P., and Castronovo, V. (1995) Galectin-1 modulates human melanoma cell adhesion to laminin. *Biochem. Biophys. Res. Commun. 209*, 760−767.
(55) van den Brule, F., Califice, S., Garnier, F., Fernandez, P. L., Berchuck, A., and Castronovo, V. (2003) Galectin-1 accumulation in the ovary carcinoma peritumoral stroma is induced by ovary carcinoma cells and affects both cancer cell proliferation and adhesion to laminin-1 and fibronectin. *Lab. Invest. 83*, 377−386.
(56) Espelt, M. V., Croci, D. O., Bacigalupo, M. I., Carabias, P., Manzi, M., Elola, M. T., Munoz, M. C., Dominici, F. P., Wolfenstein-Todel, C., Ravinovich, G. A., and Troncoso, M. F. (2011) Novel roles of galectin-1 in hepatocellular carcinoma cell adhesion, polarization, and in vivo tumor growth. *Hepatology 53*, 2097−2106.
(57) Reijngoud, D. J., and Tager, J. M. (1977) The permeability properties of the lysosomal membrane. *Biochim. Biophys. Acta 472*, 419−449.
(58) Mukherjee, S., Ghosh, R. N., and Maxfield, F. R. (1997) Endocytosis. *Physiol. Rev. 77*, 759−803.
(59) Fajka-Boja, R., Blaskó, A., Kovács-Sólyom, F., Szebeni, G. J., Tóth, G. K., and Monostori, É. (2008) Co-localization of galectin-1 with GM1 ganglioside in the course of its clathrin- and raft-dependent endocytosis. *Cell. Mol. Life Sci. 65*, 2586−2593.
(60) Sempowski, G. D., Lee, D. M., Kaufman, R. E., and Haynes, B. F. (1999) Structure and function of the CD7 molecule. *Crit. Rev. Immunol. 19*, 331−348.
(61) Pace, K. E., Hahn, H. P., Pang, M., Nguyen, J. T., and Baum, L. G. (2000) Cutting edge: CD7 delivers a pro-apoptotic signal during galectin-1-induced T cell death. *J. Immunol. 165*, 2331−2334.